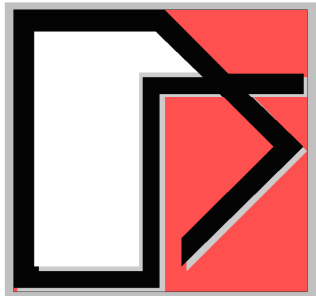


Fast Nonlinear Seismic SSI Analysis of Nuclear Structures in Complex Frequency Domain - A Breakthrough Development -



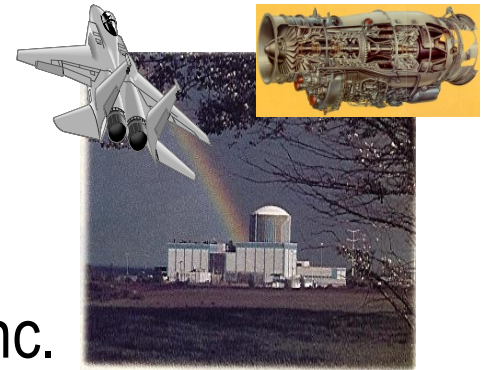
Ghiocel Predictive Technologies Inc.

Dr. Dan M. Ghiocel

Email: dan.ghiocel@ghiocel-tech.com

Phone: 585-641-0379

Ghiocel Predictive Technologies Inc.



GP Tech Rochester Office, New York, USA

October 1, 2013

Purpose of This Presentation:

The presentation shows a novel nonlinear SSI approach for modeling of nonlinear hysteretic behaviors of reinforced concrete structures in the complex frequency domain.

The new approach can be used to perform fast and accurate nonlinear SSI analyses, including sophisticated nonlinear hysteretic models, at a small fraction of the runtime of a time domain nonlinear SSI analysis.

A case study of a nuclear shearwall building is presented in relative detail.

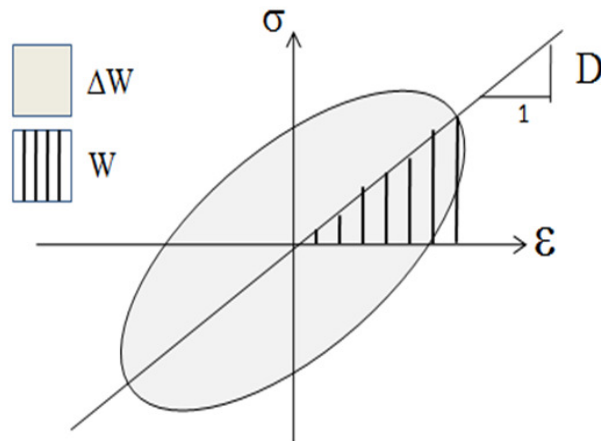
ACS SASSI Option N was used for nonlinear SSI analysis.

Equivalent-Linear System in Complex Frequency

Based on the up-to-date literature, the nonlinear behavior of dynamic structural systems can be captured only by nonlinear time history analyses.

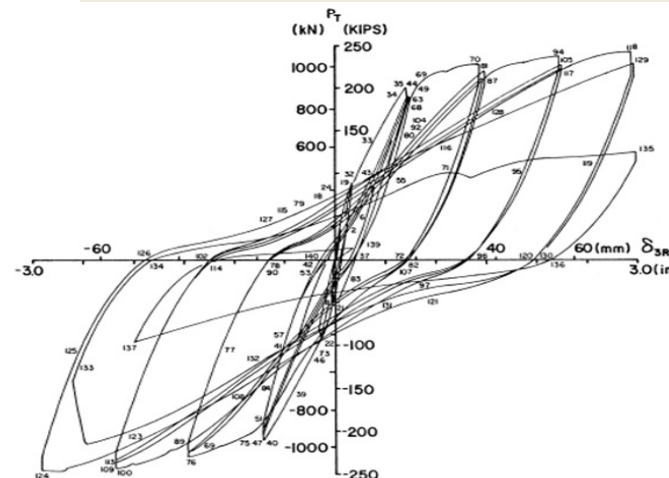
Only simple equivalent linear (EQL) approaches were applied in frequency domain. As a result of the EQL model *time invariant behavior*, the SSI response could be either over or under estimated at different time moments.

Linear Hysteretic Model



Frequency Domain
(Time-Invariant System)
(Frequency-Invariant)

Non-Linear Hysteretic Model



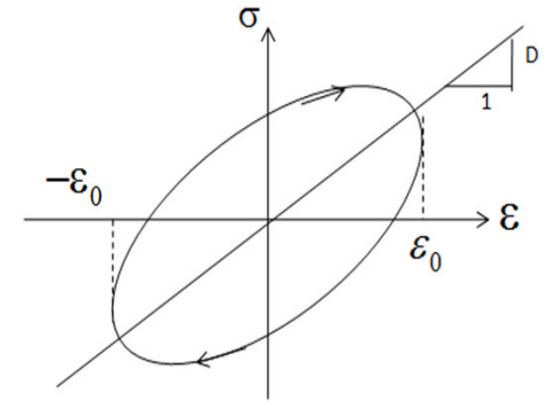
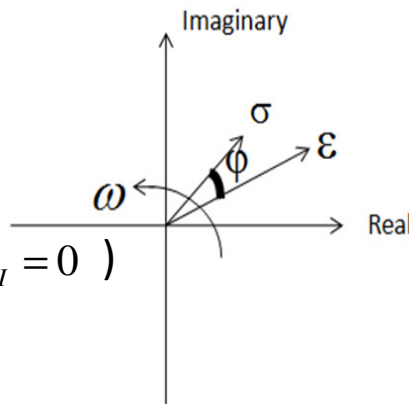
Time Domain
(Time-Dependent System)
(Frequency-Dependent)

Linear Hysteretic (Voigt) Model in Complex Frequency

In complex frequency, Hooke Law is:

$$\sigma^*(\omega) = D^*(\omega)\epsilon^*(\omega)$$

$$D^*(\omega) = D_R + iD_I \text{ (for elastic solid } D_I = 0 \text{)}$$



Visco-Elastic Material Model

$$\beta = \frac{1}{4\pi} \frac{\Delta W}{W}$$

$$D^* = D_R \left(\begin{array}{l} 1 - 2\beta^2 \\ \text{real part} \end{array} + 2i\beta \sqrt{1 - \beta^2} \right) \left(\begin{array}{l} \\ \text{imag part} \end{array} \right)$$

In time domain, using Fourier duality:

$$\sigma(t) = \sigma_{elast}(t) + \sigma_{diss}(t)$$

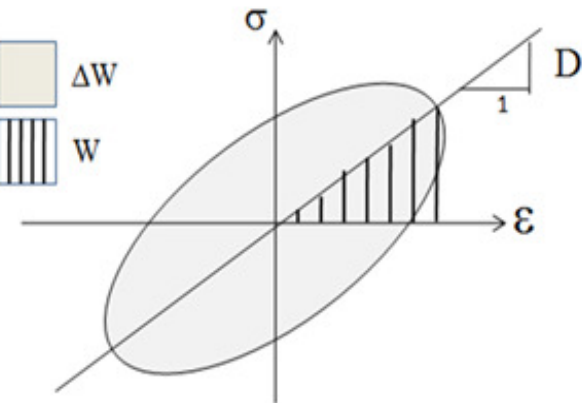
$$\sigma_{elast}(t) = \frac{1}{2\pi} \int_{-\infty}^{\infty} D_R(\omega) \epsilon^*(\omega) \exp(-i\omega t) d\omega$$

$$\sigma_{diss}(t) = \frac{1}{2\pi} \int_{-\infty}^{\infty} D_I(\omega) \epsilon^*(\omega) \exp(-i\omega t) d\omega$$

Energy Loss



Strain Energy



Using Fourier duality linear (nonlinear) time response can be mapped in a complex frequency response and vice-versa.

Nonlinear Hysteretic Models in Time and Frequency

To map a linear system response time history we need a linear (frequency-independent) hysteretic model.

To map a nonlinear system response time history we need a nonlinear (frequency-dependent) hysteretic model.

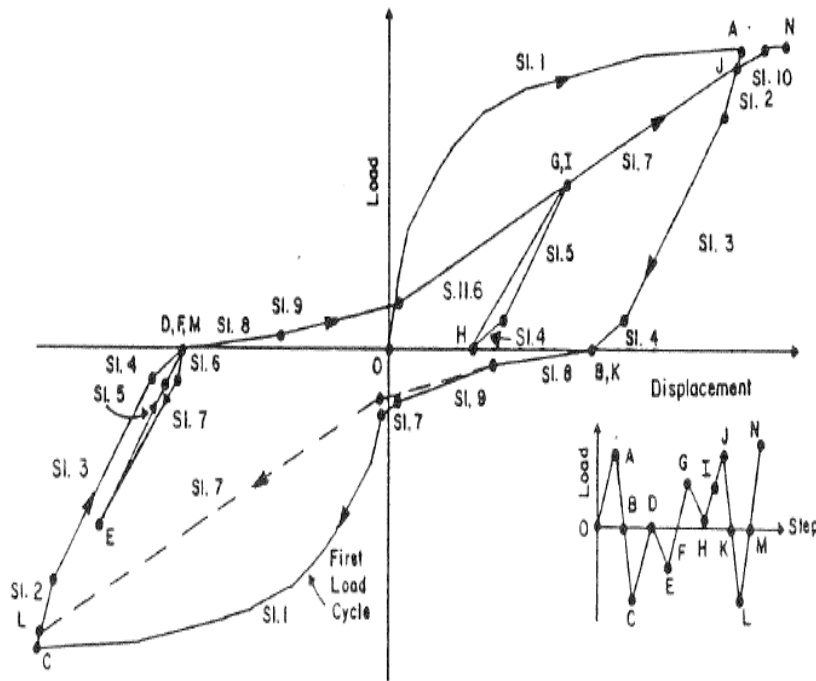
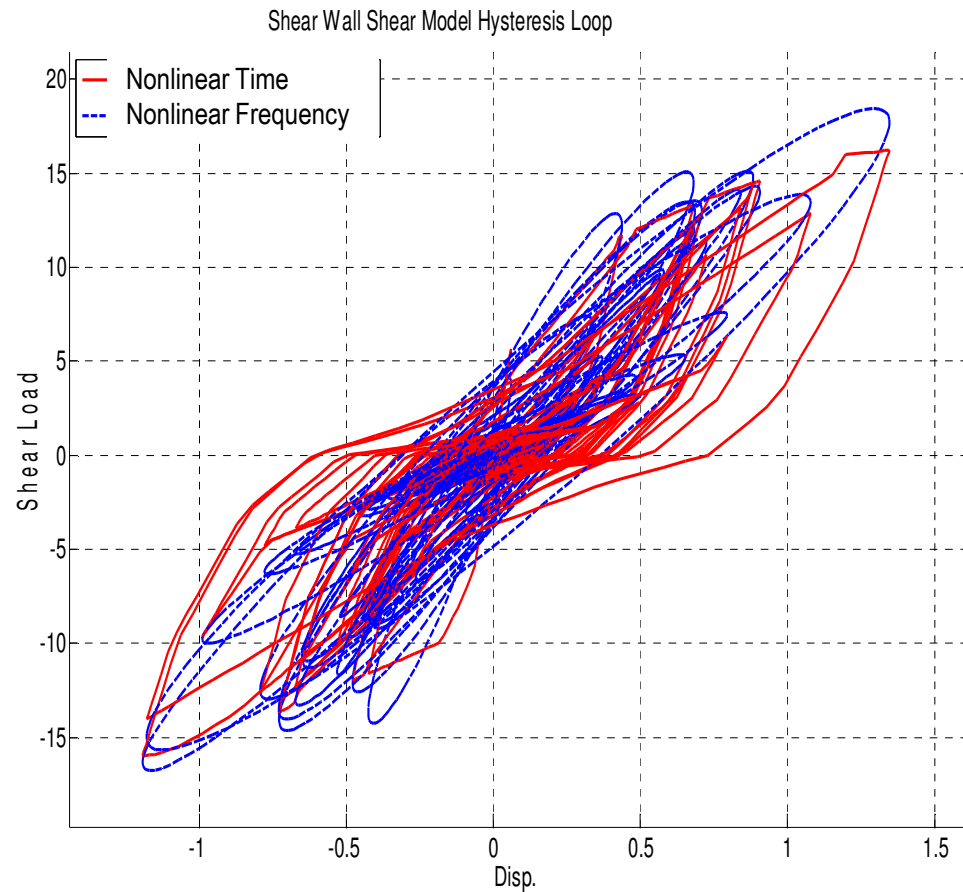
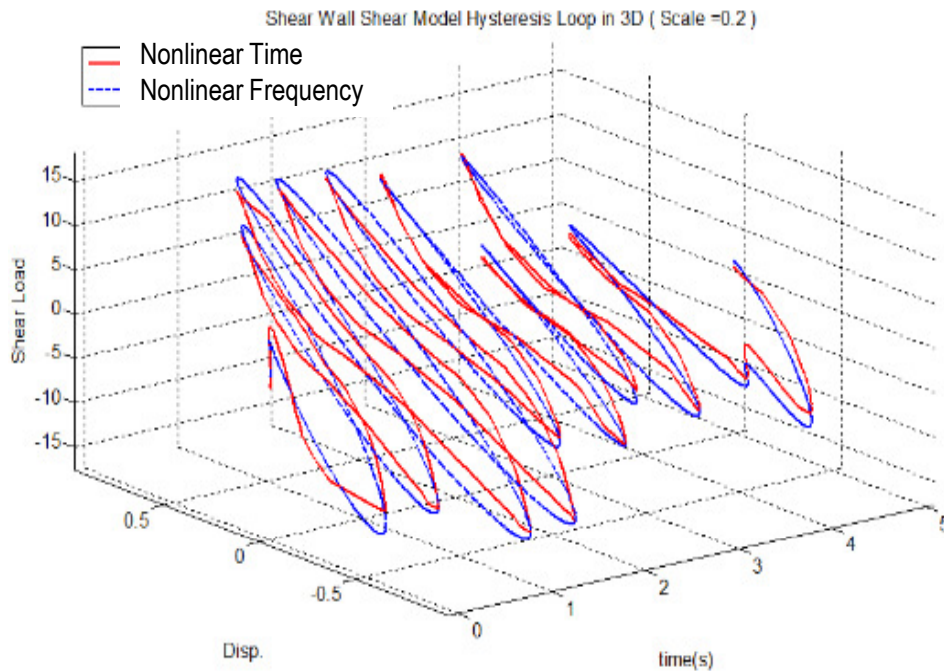


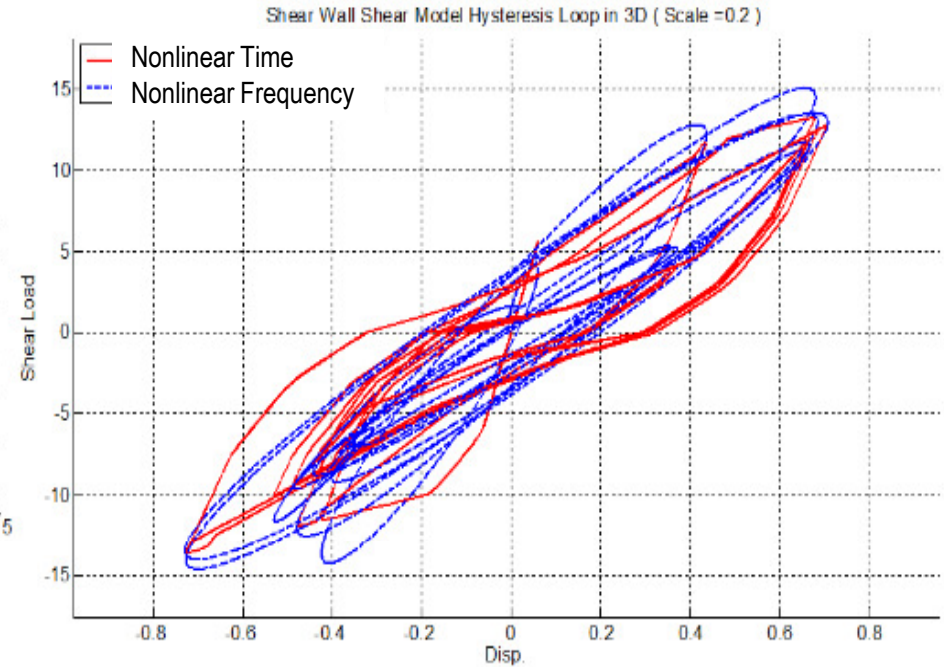
Figure 5b. Shear hysteresis model



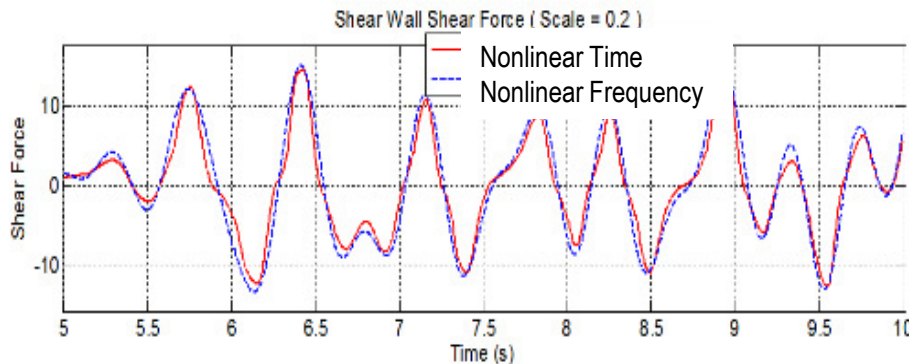
Nonlinear Hysteretic Model in Complex Frequency



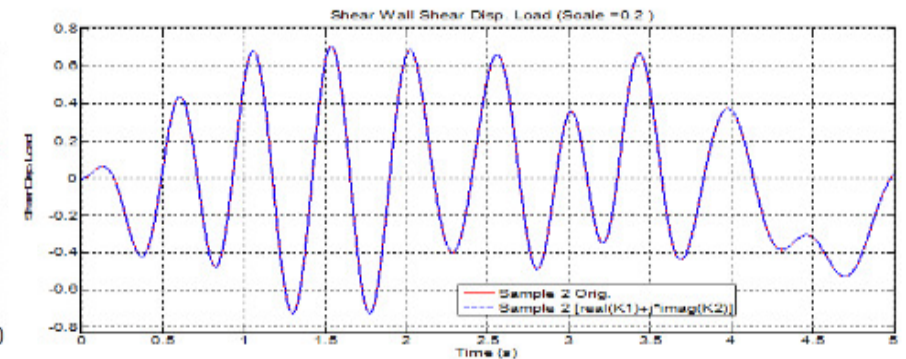
Comparison Hysteretic Loops in Time-Domain



Comparison of the Two Nonlinear Hysteretic Models



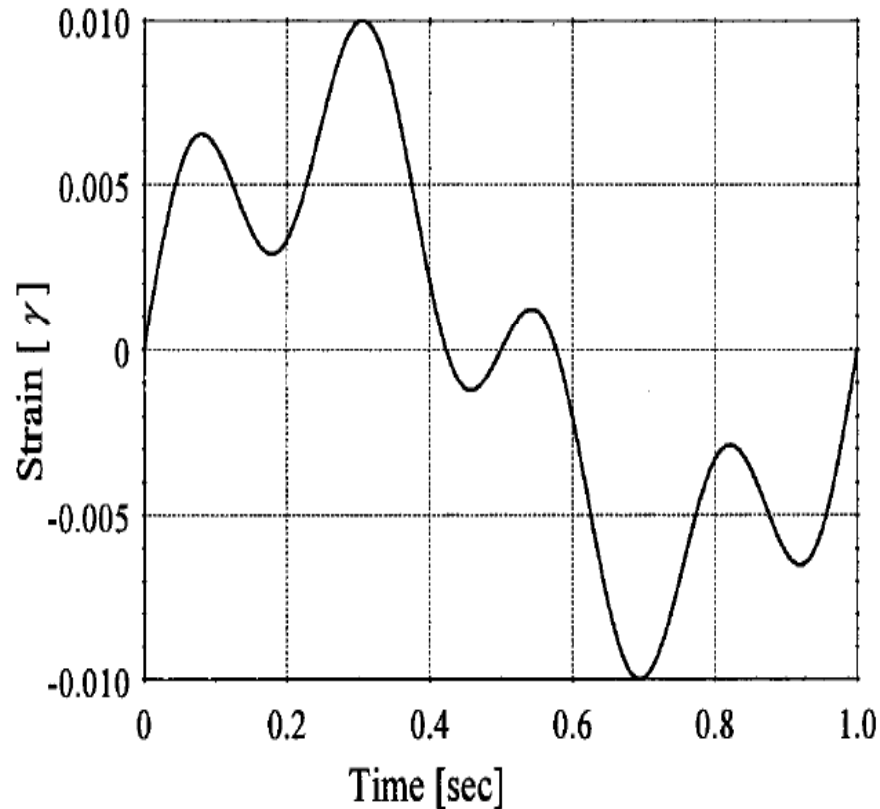
Shear force in time



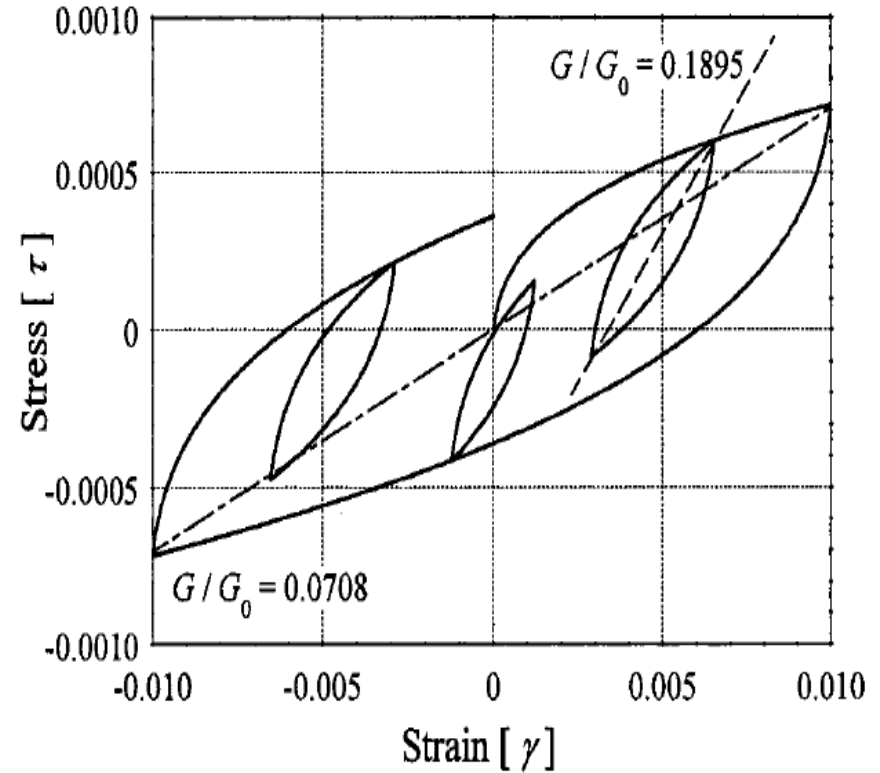
Displacement

Frequency-Dependent Linearized Hysteretic Models in Complex Frequency: Kausel-Assimaki Model

Time Response

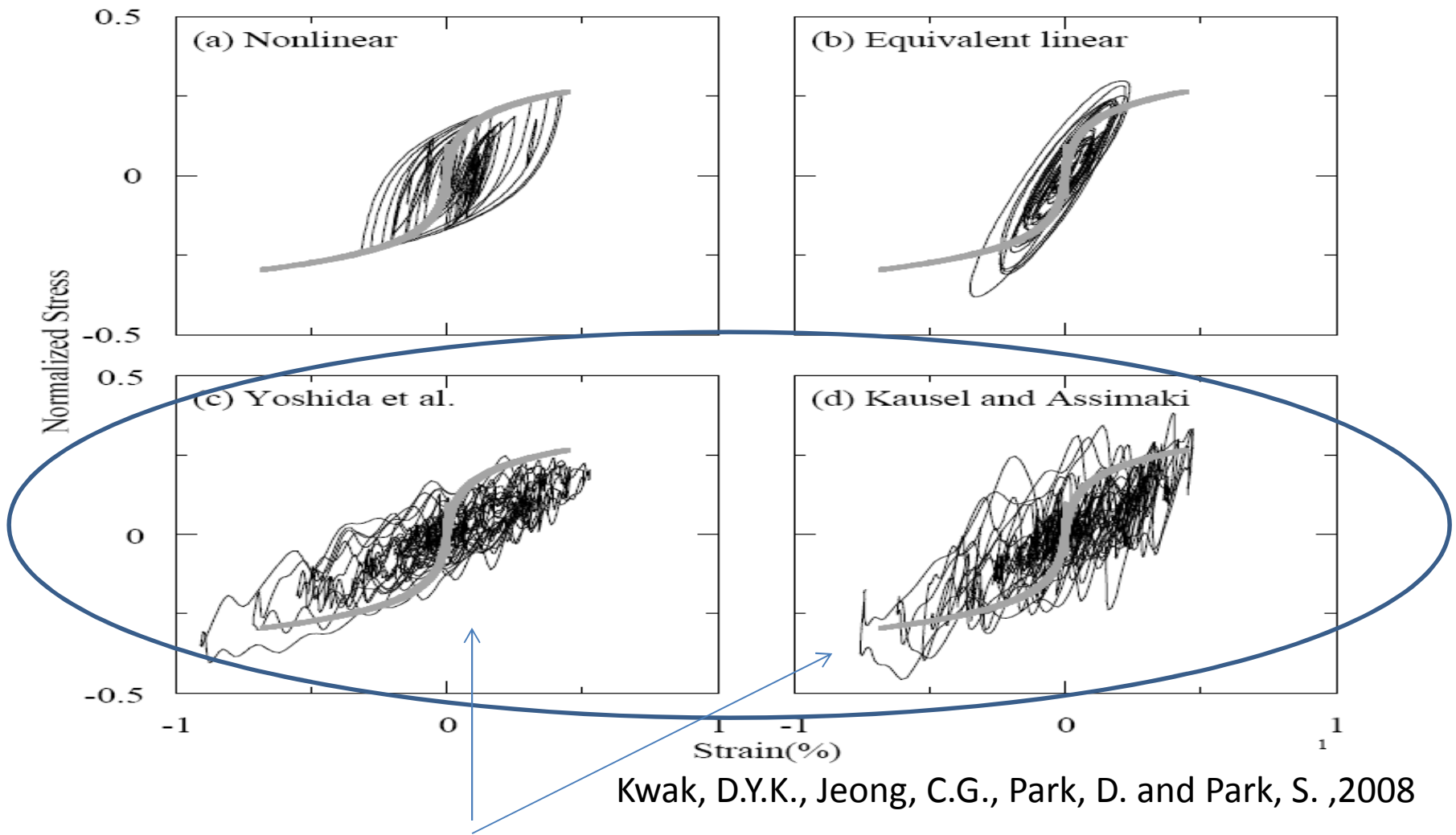


Hysteretic Loops



Kausel, E. and Assimaki, D., 2002

Frequency-Dependent Hysteretic Model Results



Kwak, D.Y.K., Jeong, C.G., Park, D. and Park, S. ,2008

REMARK: Kausel and Assimaki (2002) and Yoshida et al. (2002) implementations lacked in the compatibility between the frequency and the time domain representations.

Nonlinear Plasticity FEA Models: ANACAP Model

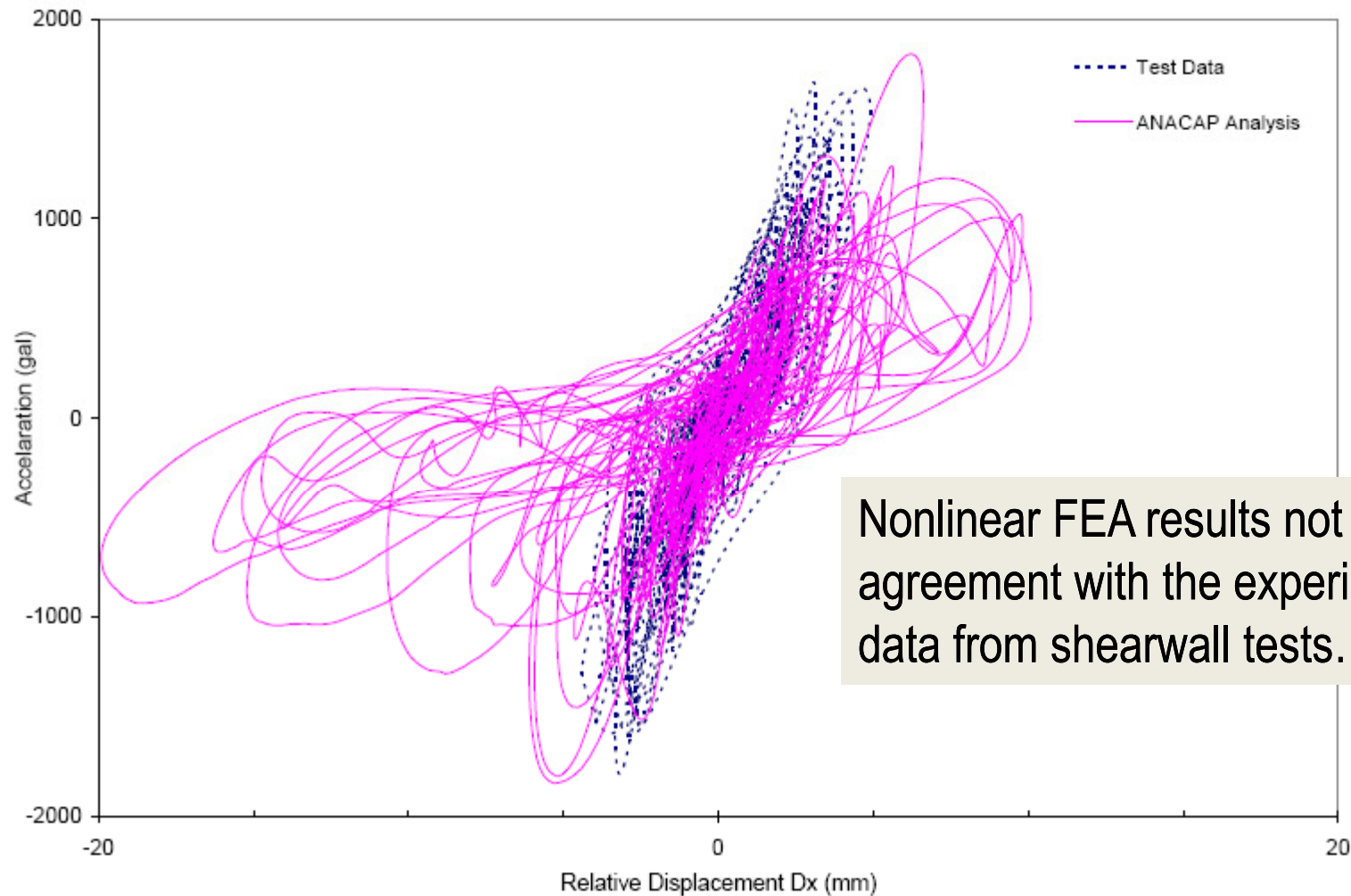


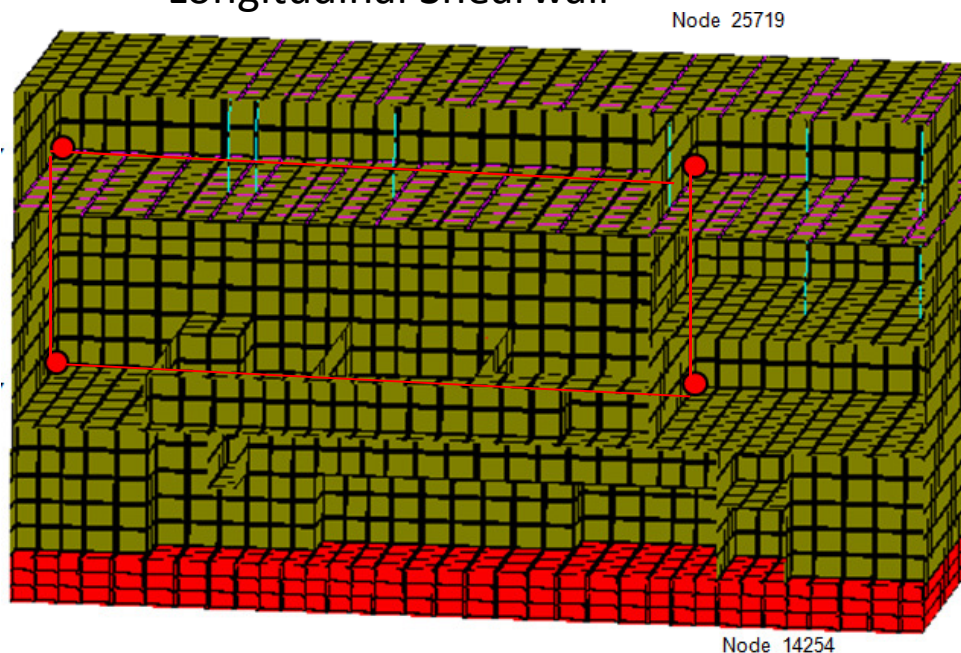
Figure 5-86 Comparison of X-Direction Hysteresis from ANACAP Analysis Considering Prior Damages but with X-Input Motion only and Test Result for Run-6

NUREG/CR-6925, BNL-NUREG-77370, 2006

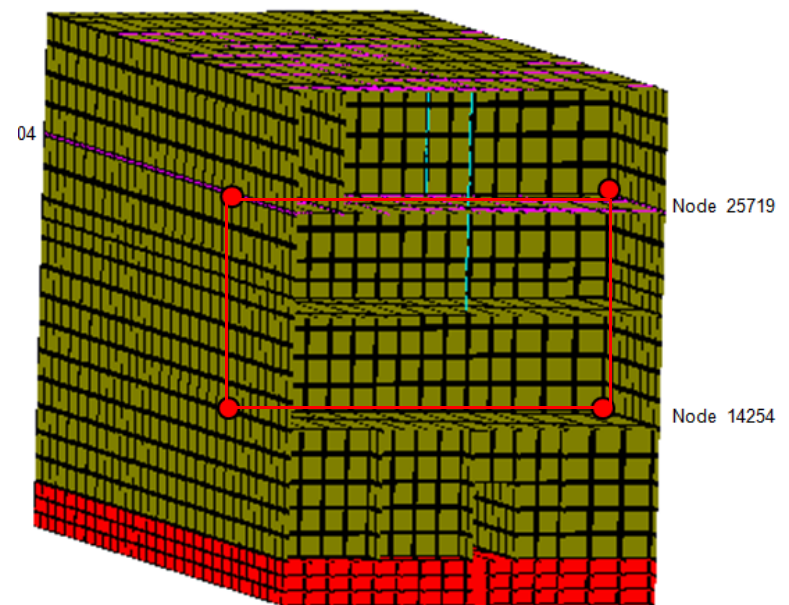
Nonlinear SSI Analysis of Low-Rise Shearwall Buildings

- Define shearwall panels between floors that will behave nonlinear.
- Define shearwall panel back-bone curves and hysteretic models based on experimental evidence, in accordance with recommendations of ASCE 43-2005 and ASCE 41-06.

Longitudinal Shearwall



Transverse Shearwall



Nonlinear SSI Analysis in Complex Frequency:

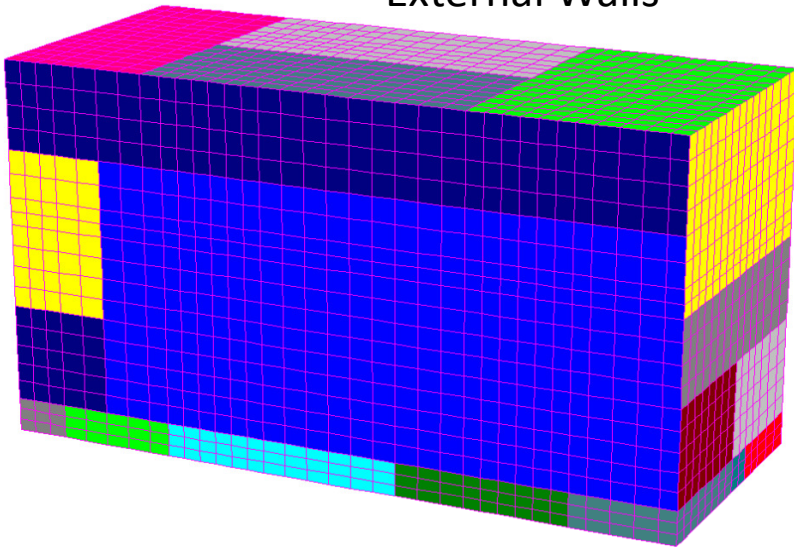
Computational Steps:

- For the initial iteration, perform a linear SSI analysis using the elastic properties for the selected shearwall panels
- Compute the reinforced concrete shearwall panel behavior in time domain and frequency domain using the hysteretic model associated to each selected panel
- Perform a new SSI analysis iteration using a fast SSI reanalysis (restart analysis) in the complex frequency domain using the hysteretic models computed in Step 2 for all selected panels
- Check convergence of the nonlinear SSI response after new SSI iteration, and go back to Step 2 if the convergence was not achieved.

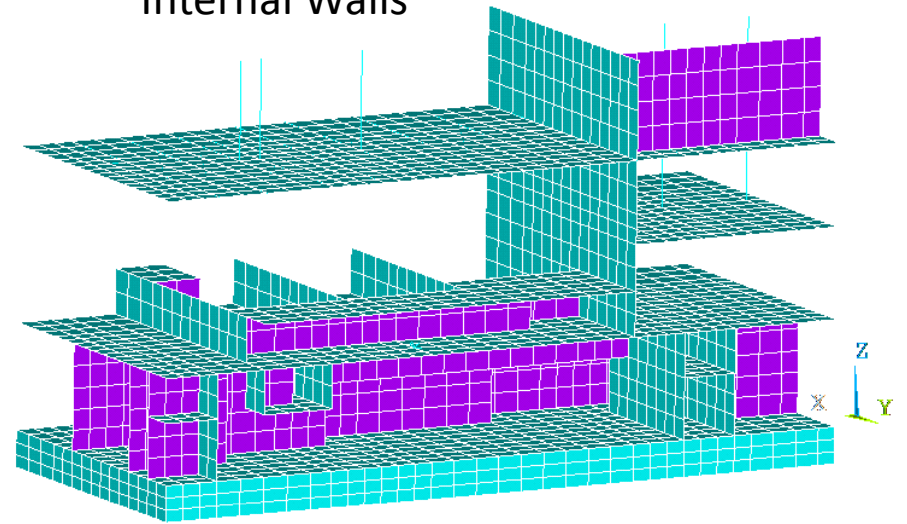
Nuclear Shearwall Building on A Rock Site



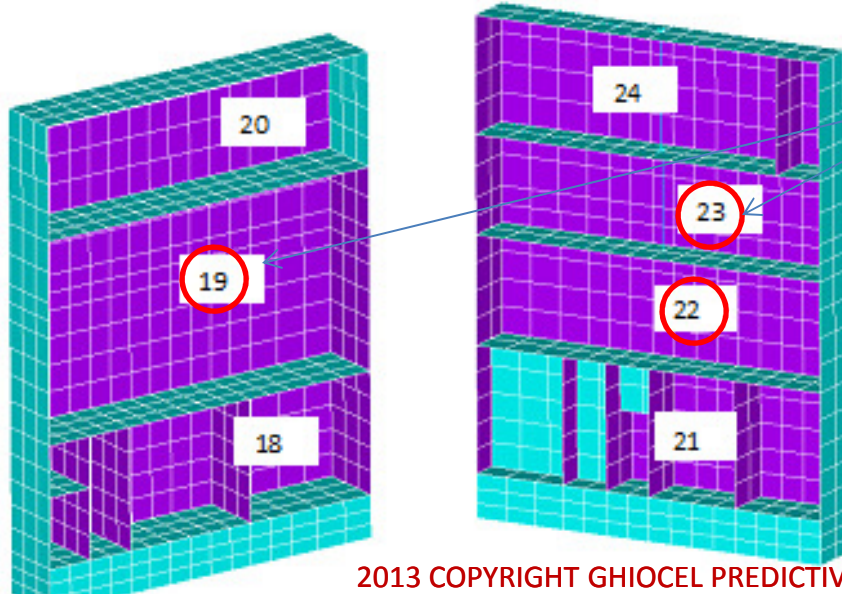
External Walls



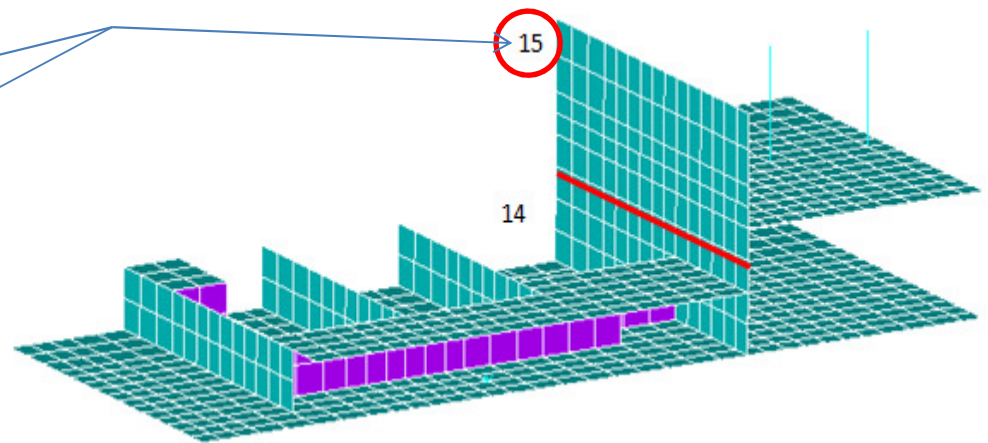
Internal Walls



Transverse External Walls



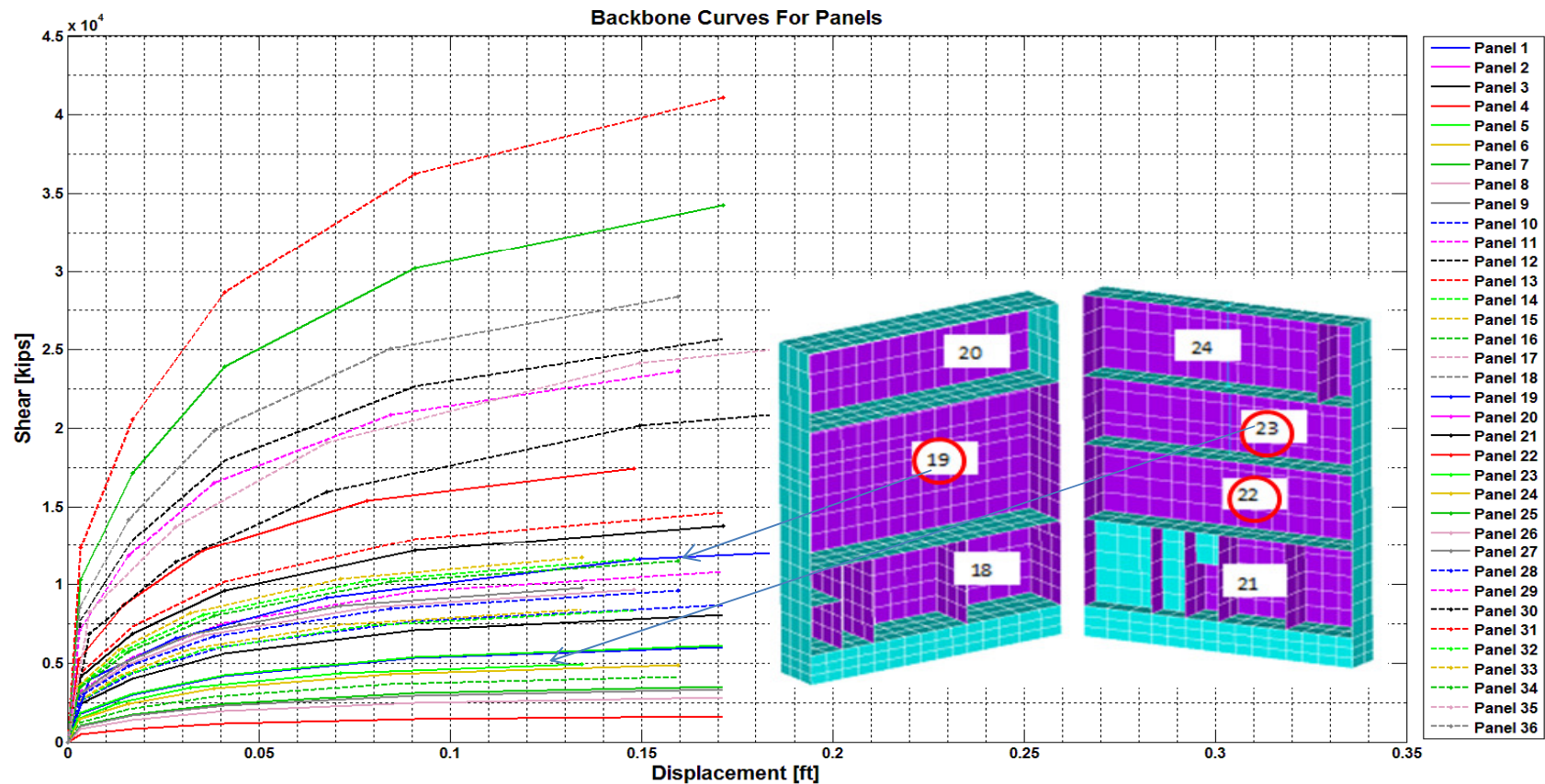
Transverse Internal Walls



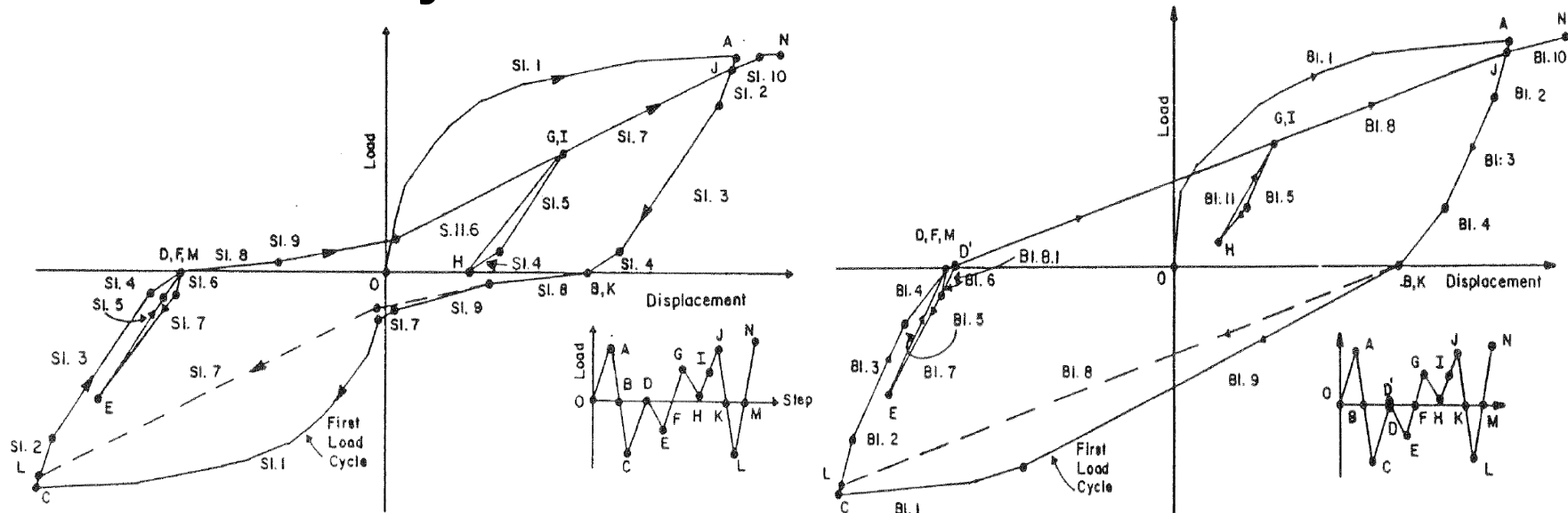
Shearwall Back Bone Curves (BBC) for All Shearwalls

A number of 36 wall panels were modeled for nonlinear SSI analysis.
For each BBC were determined based on ASCE 04-2013 and ASCE 43-05.

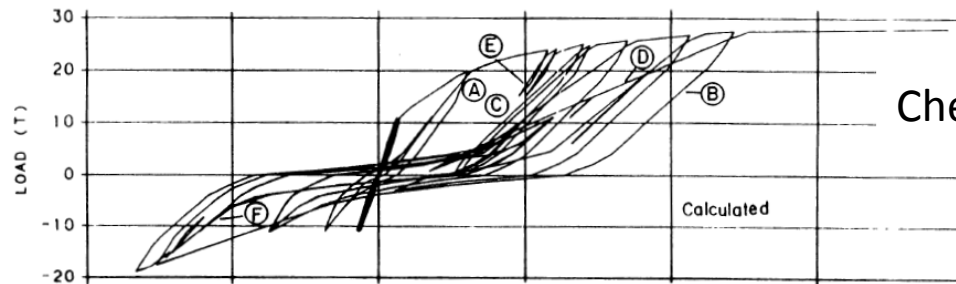
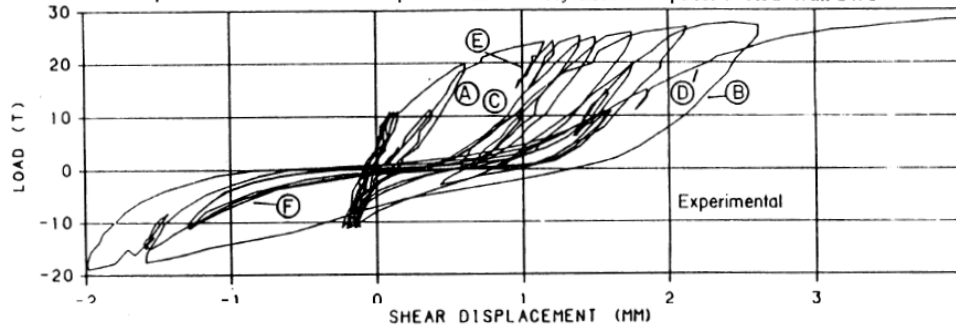
Focus of the weak story (results shown for the panels #19 and 23)



Chen-Mertz Hysteretic Model for Low-Rise Shearwalls



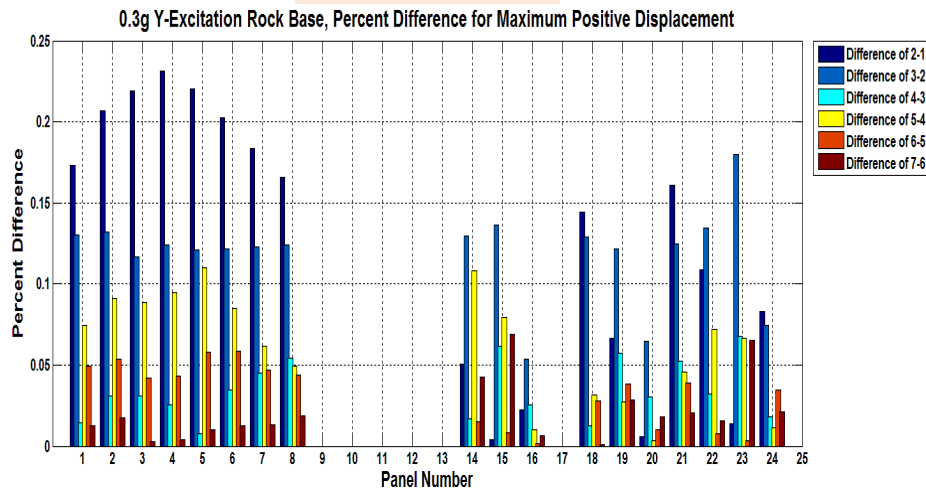
Comparison of Calculated and Experimental Shear Hysteresis Loops for NCKU Wall SW6



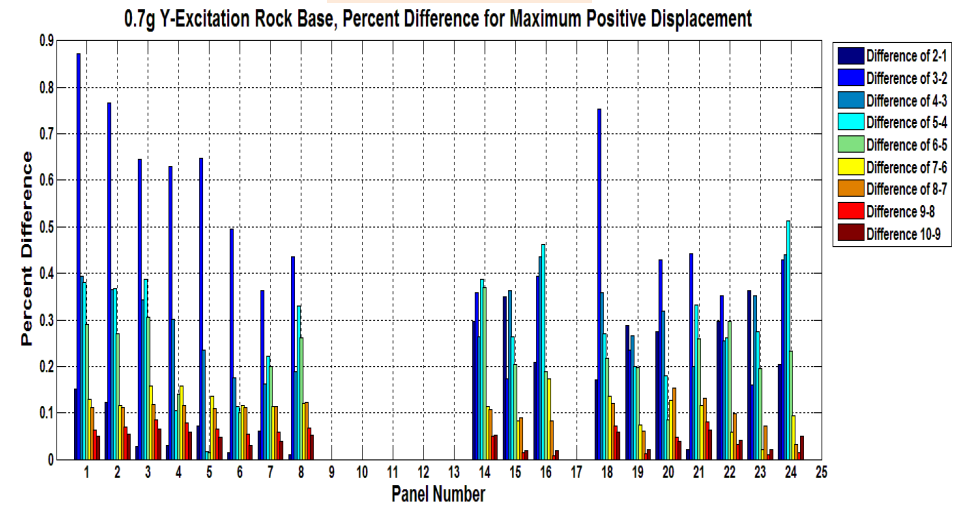
Cheng and Mertz, 1989

Nonlinear SSI Analysis Convergence (Per Panel and Global)

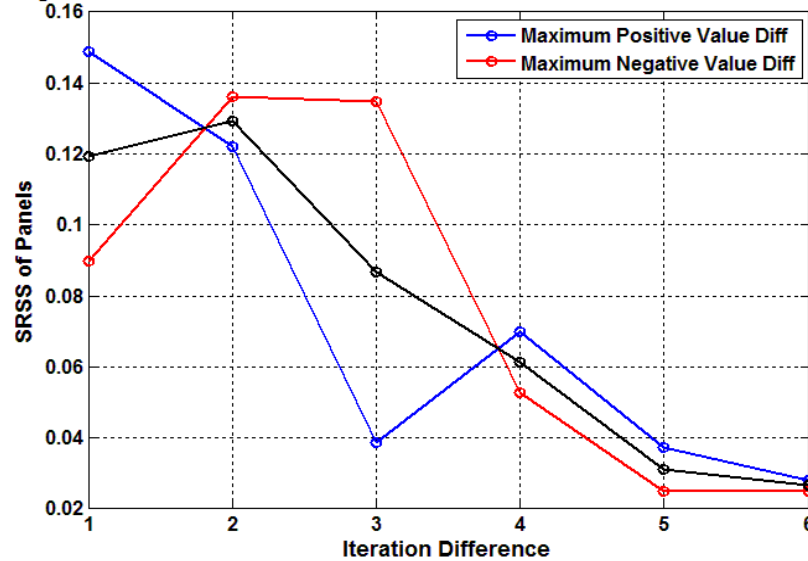
0.30g ZPGA



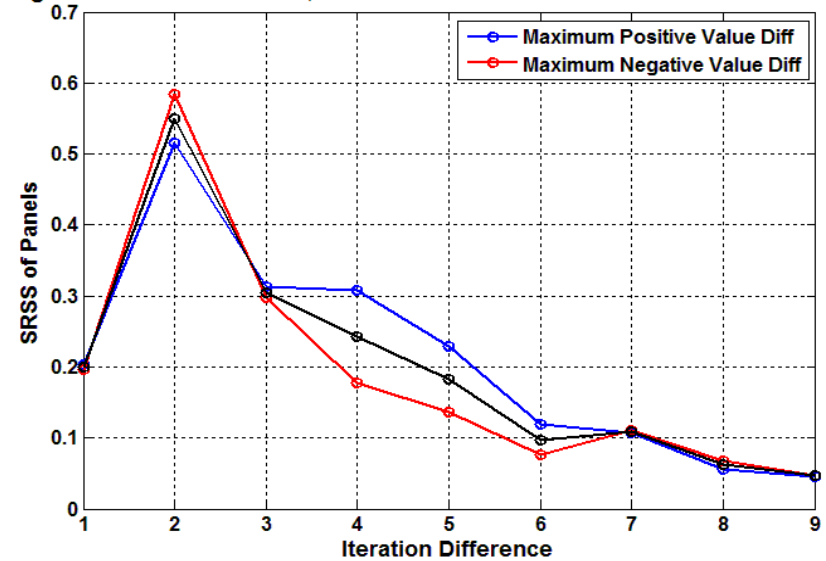
0.70g ZPGA



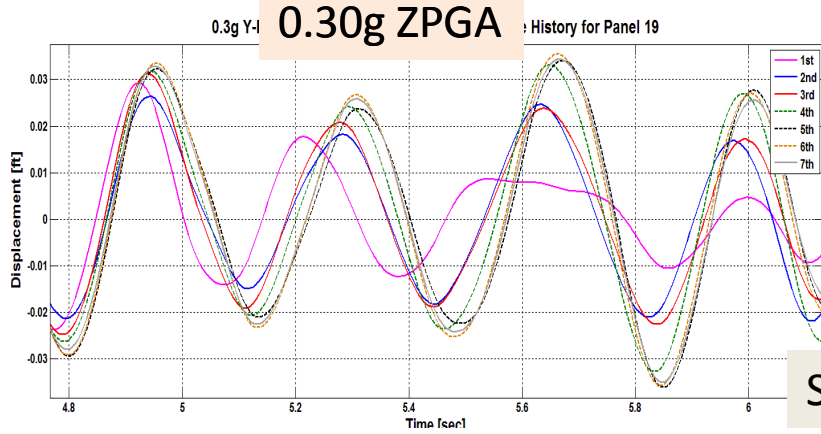
0.3g Y-Excitation Rock Base, SRSS of Difference Between Iterations for All Panels



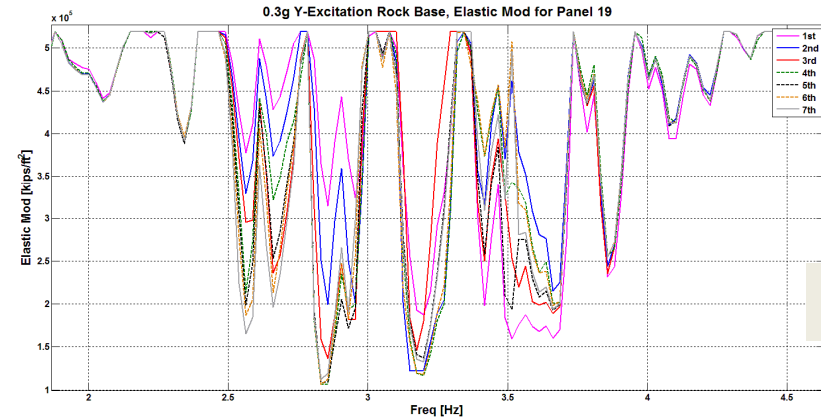
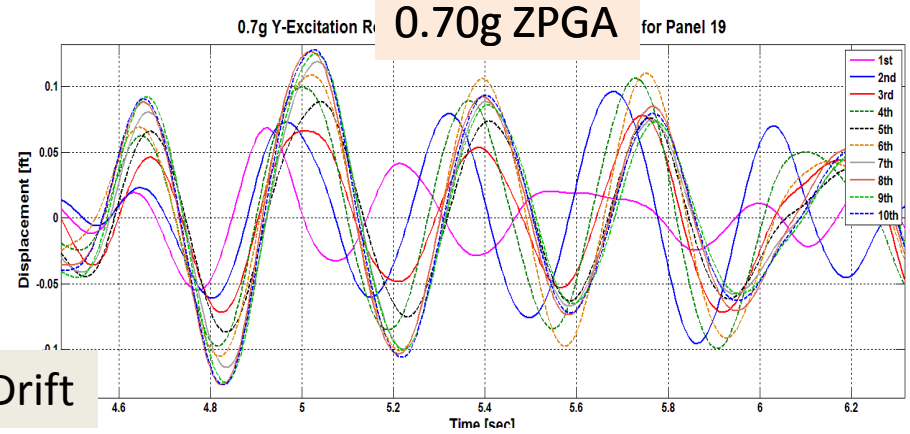
0.7g Y-Excitation Rock Base, SRSS of Difference Between Iterations for All Panels



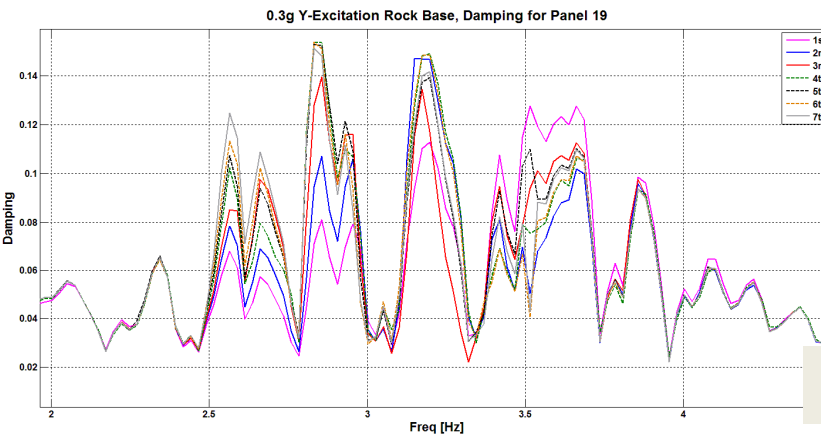
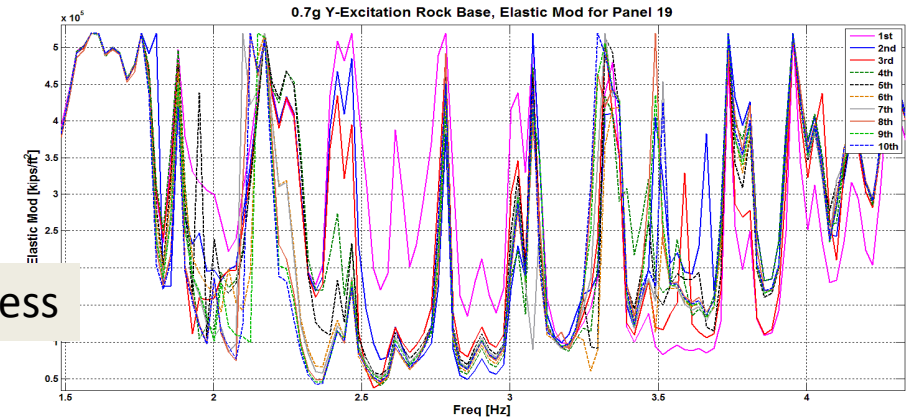
Nonlinear SSI Analysis Iteration History for Panel # 19



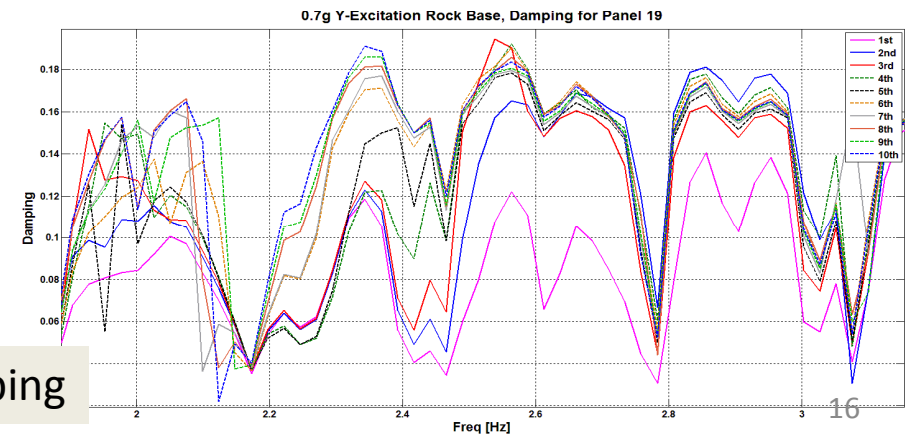
Story Drift



Stiffness



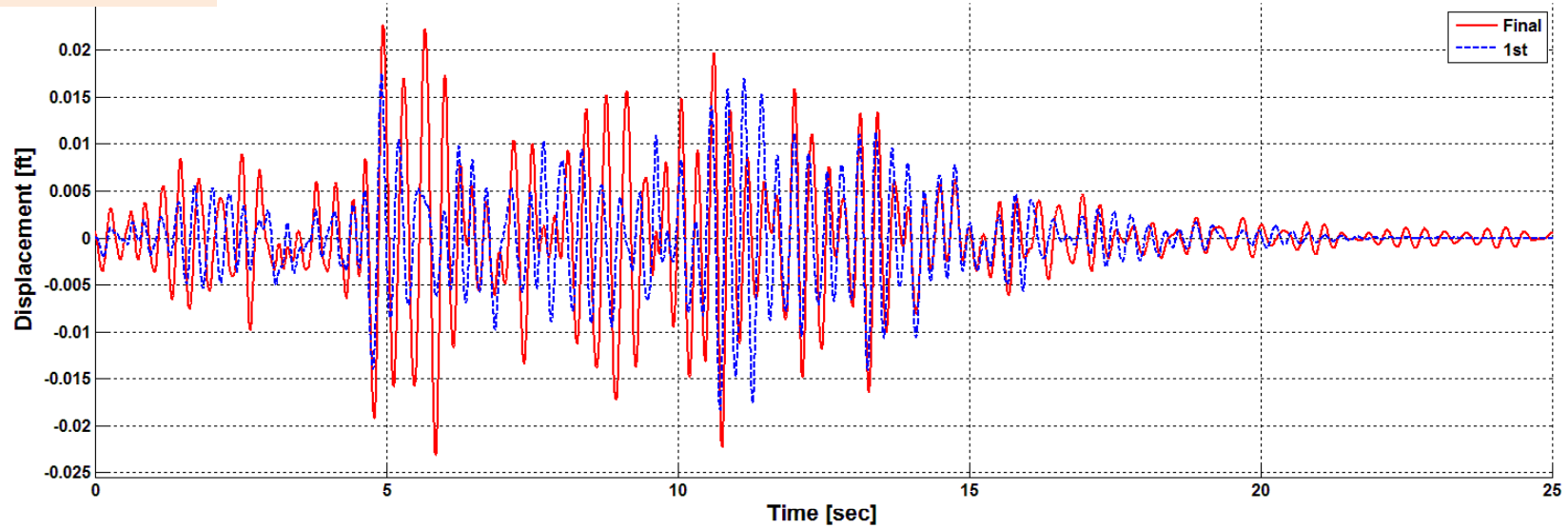
Damping



Panel #23 Comparative Linear and Nonlinear Story Drifts

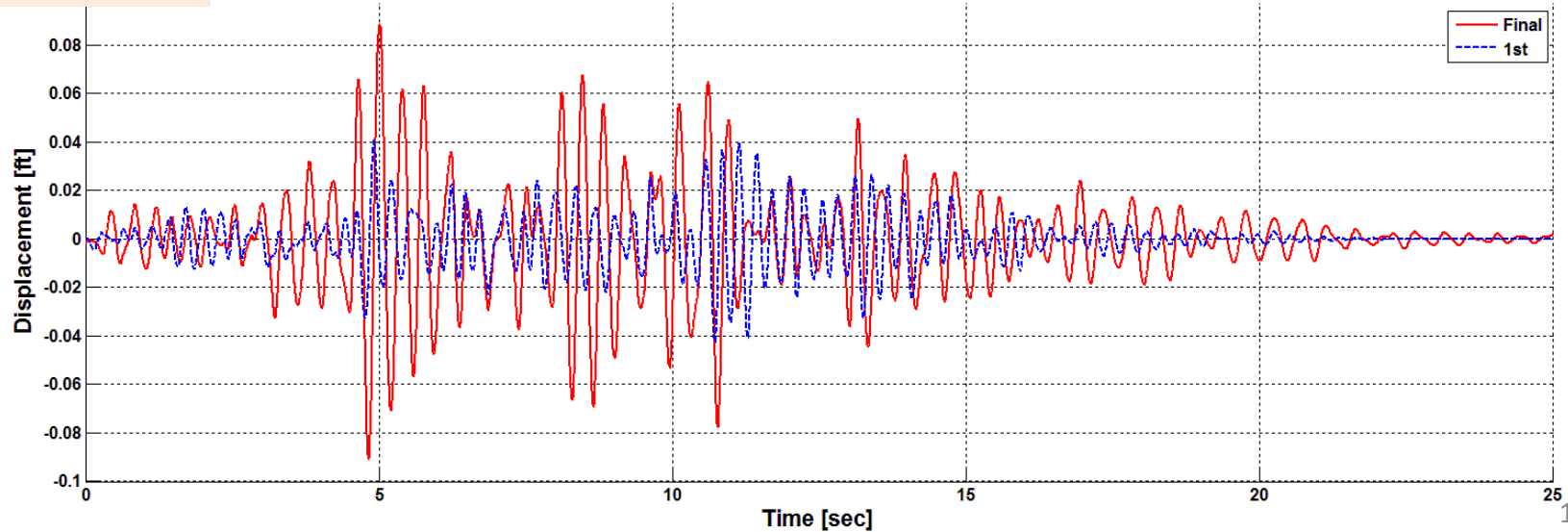
0.30g ZPGA

Y 0.3g Rock Base, Displacement Time History for Panel 23, for Initial and Final Iterations

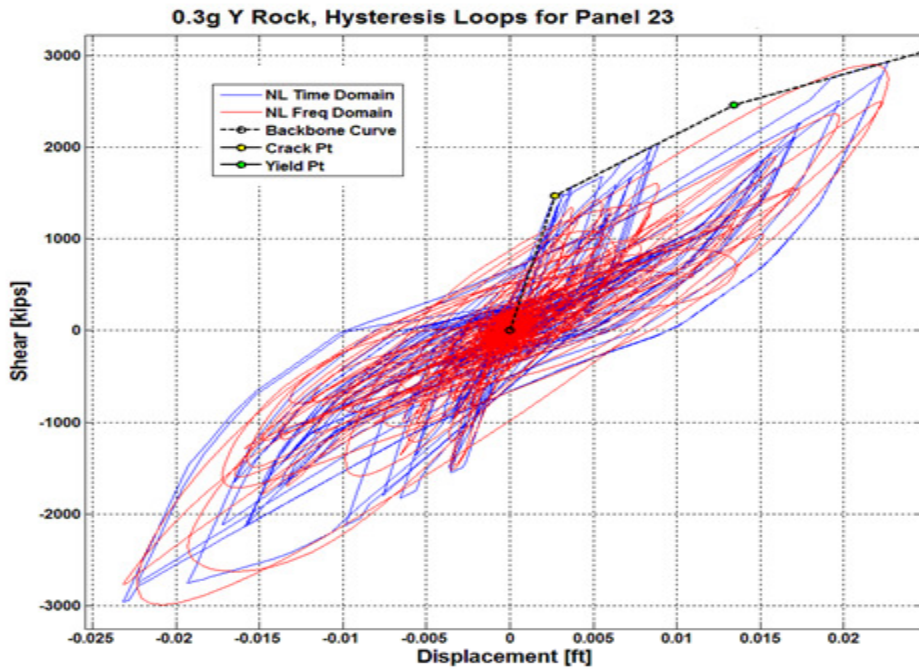


0.70g ZPGA

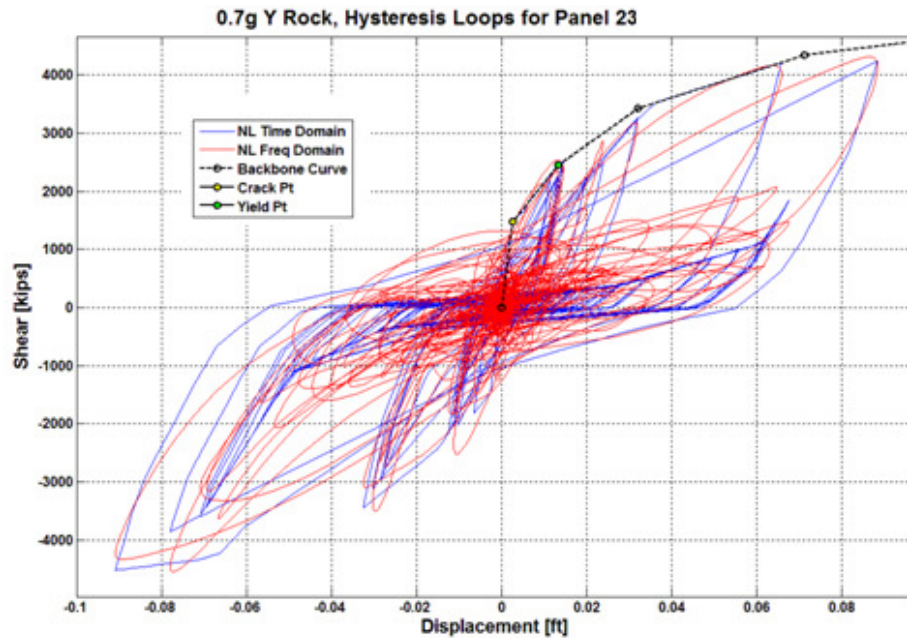
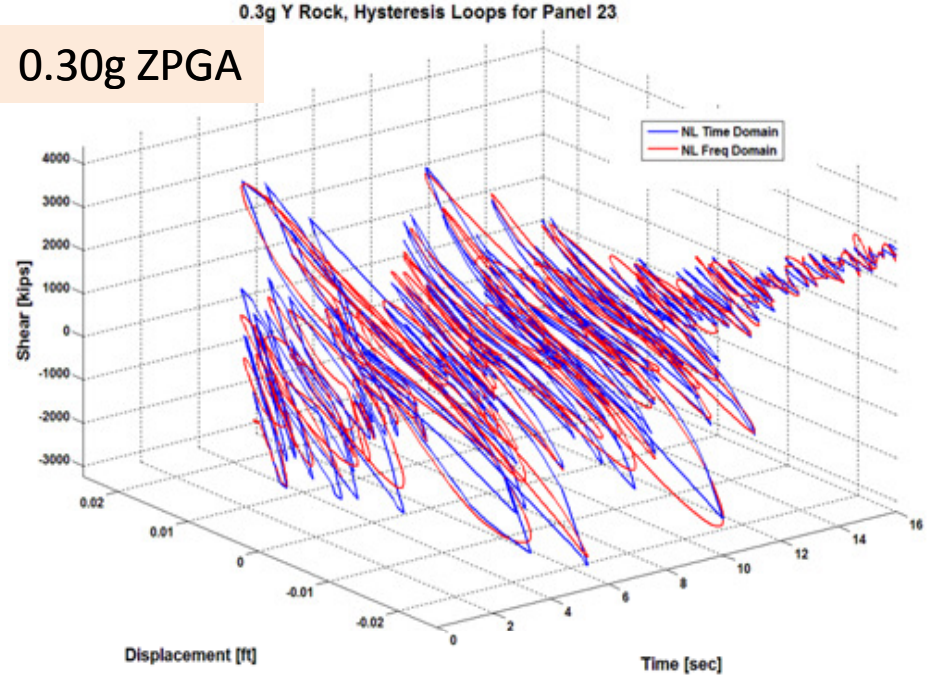
Y 0.7g Rock Base, Displacement Time History for Panel 23, for Initial and Final Iterations



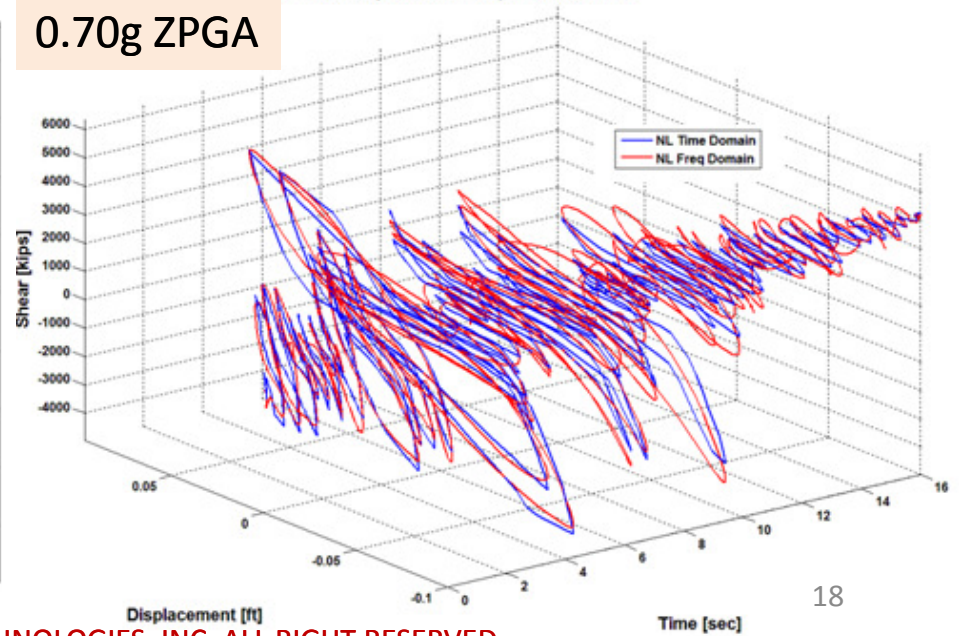
Panel #23 Hysteretic Loops for 1st and Final Iterations



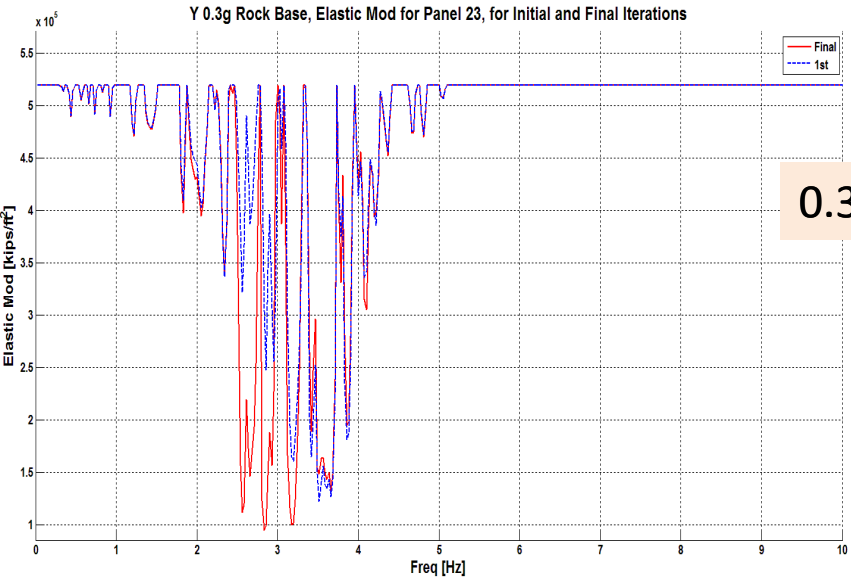
0.30g ZPGA



0.70g ZPGA

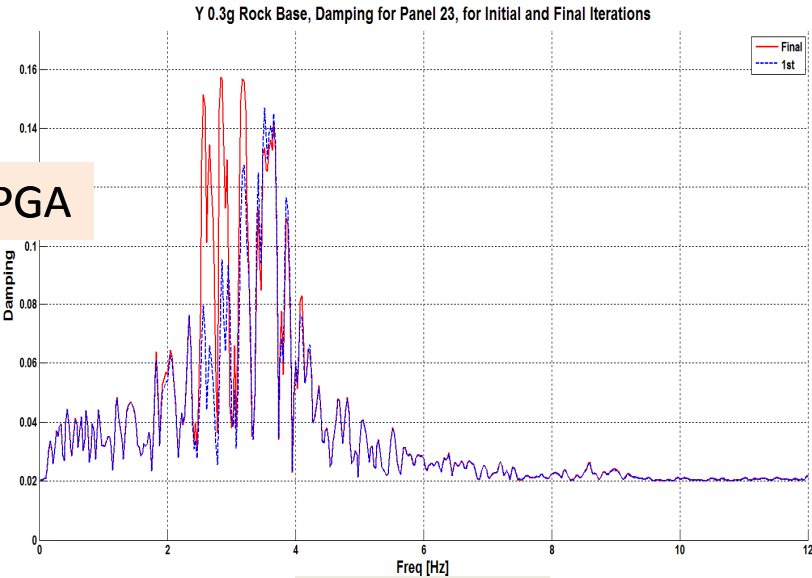


Panel #23: Frequency-Dependent Stiffness and Damping

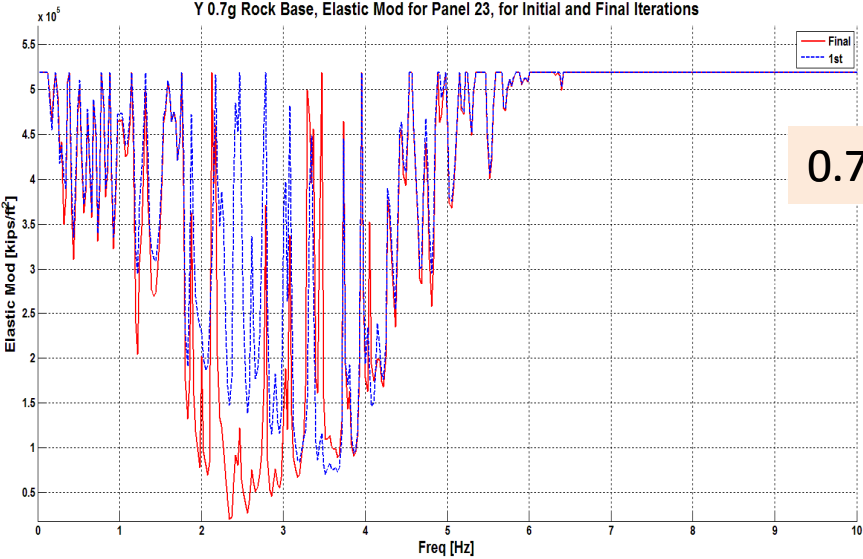


0.30g ZPGA

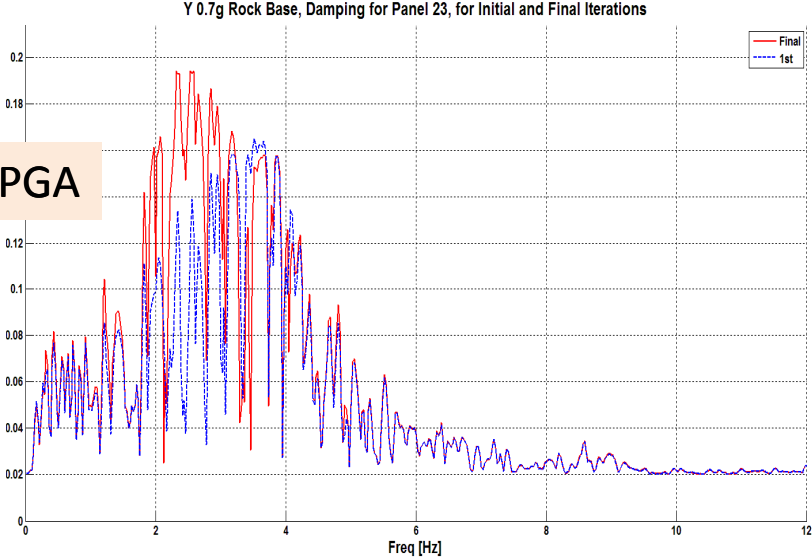
Stiffness



Damping

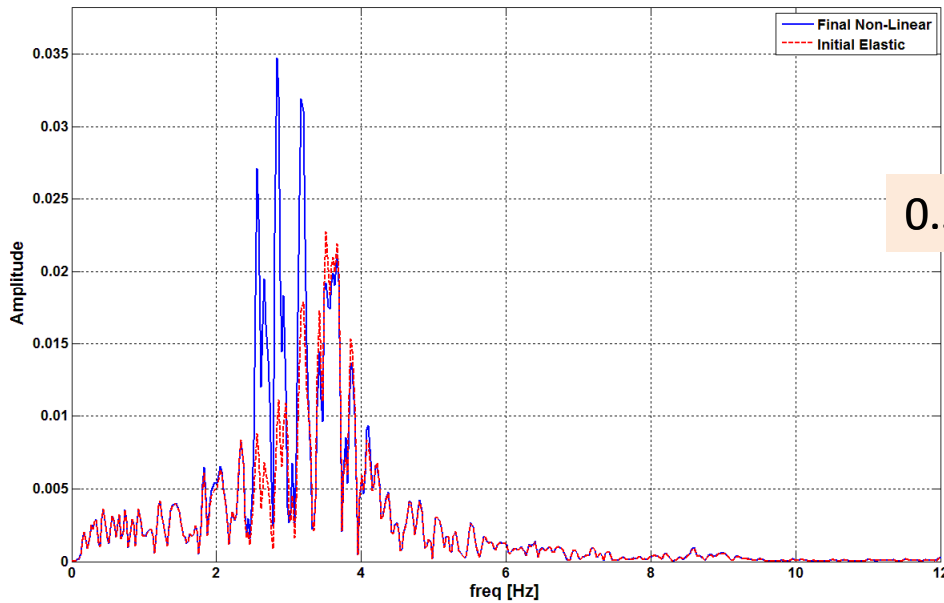


0.70g ZPGA



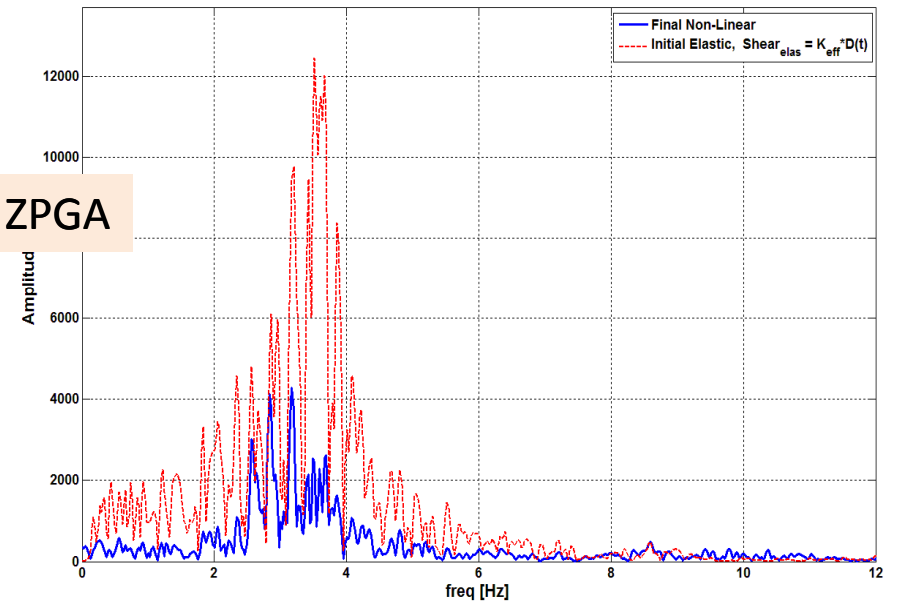
Panel #23: Amplitude Fourier of Story Drifts and Shear Forces

0.3g Y Rock, Displacement Amplitudes for Panel 23



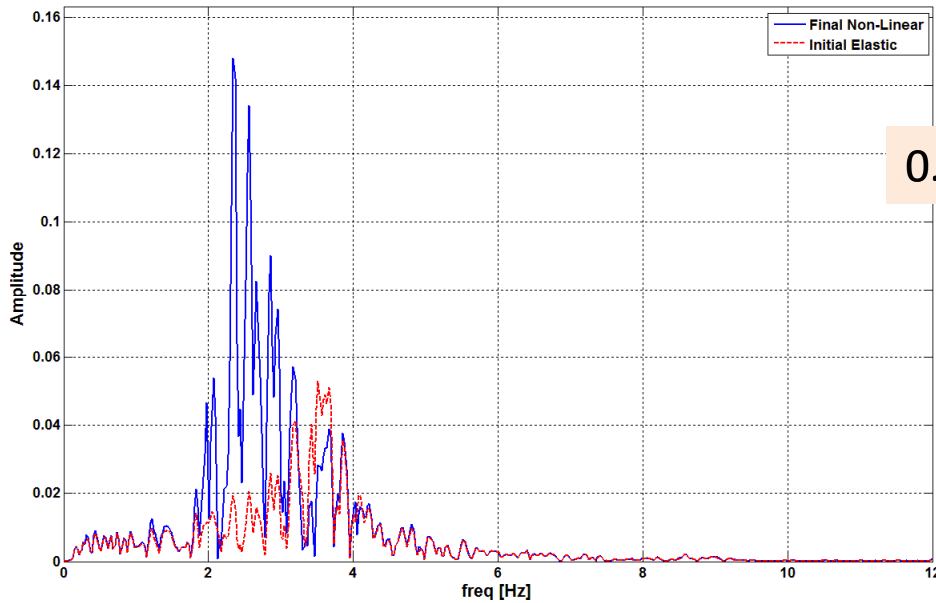
0.30g ZPGA

0.3g Y Rock, Shear Amplitudes for Panel 23



Story Drift Fourier Amplitude

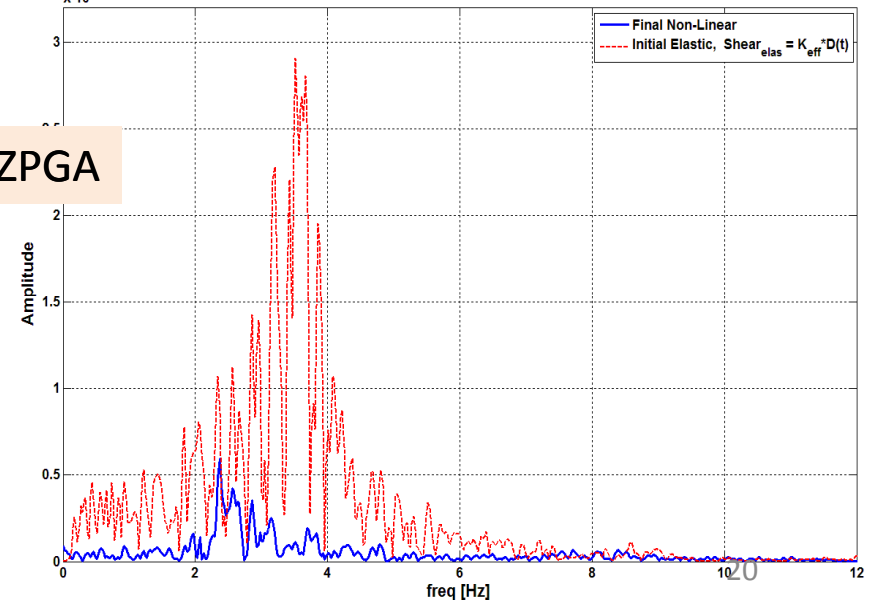
0.7g Y Rock, Displacement Amplitudes for Panel 23



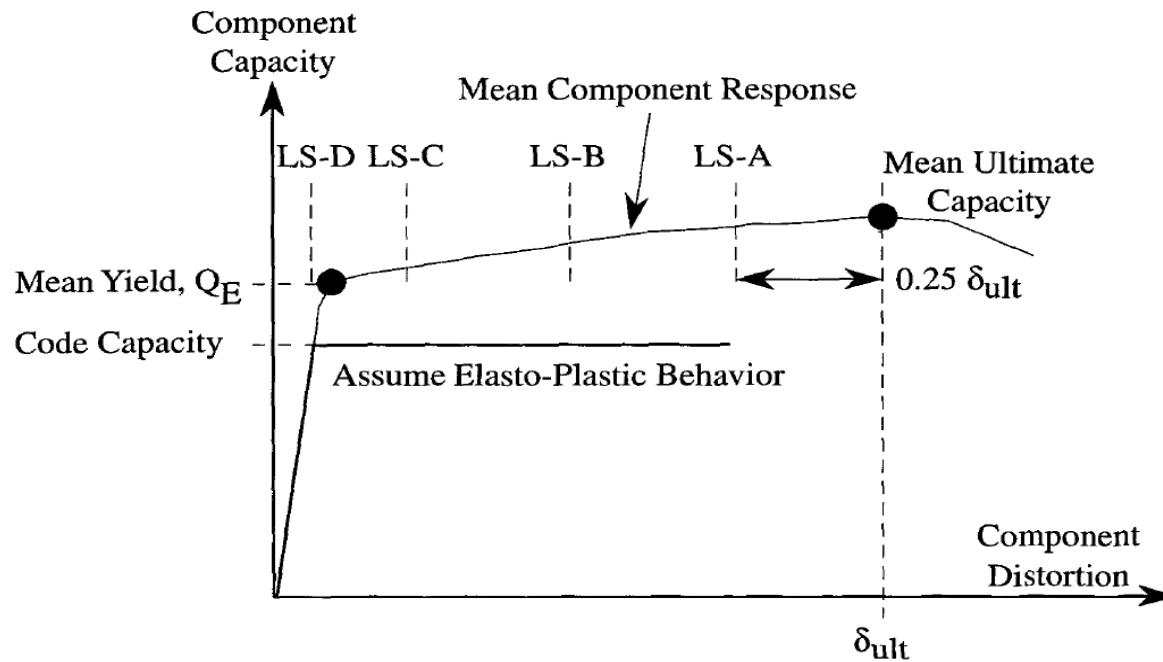
0.70g ZPGA

Shear Force Fourier Amplitude

0.7g Y Rock, Shear Amplitudes for Panel 23



ASCE 43-05 Inelastic Reduction Factors for Different Damage States



C5-4 Typical Load-Deformation Curve and Limit States

Limit State	LS-A	LS-B	LS-C
SMRF reinforced concrete moment frames			
Beams $(15 \leq \ell/h)$	5.25	4.0	2.5
Beams $(\ell/h \leq 10)$	3.25	3.0	2.5
Columns**	2.0	1.75	1.5
Reinforced concrete shear wall, in plane:			
Bending controlled walls, $\frac{h_w}{\ell_w} \geq 2.0$			
$6\sqrt{f'_c} < f_v$	2.25	2.0	1.75
$f_v < 3\sqrt{f'_c}$	2.5	2.25	1.75
Shear controlled walls, $\frac{h_w}{\ell_w} < 2.0$	2.0	1.75	1.5

Nonlinear SSI and ASCE 43-05 Inelastic Reduction Factors

0.30g ZPGA Design Level (LS-D)

Panel Number	ASCE 43		Calcs
	μ , Final Analysis	$F\mu$, Final Analysis	$F\mu$, Shear
1	0.716	0.657	1.042
2	0.662	0.568	1.004
3	0.664	0.573	1.029
4	0.734	0.684	1.097
5	0.776	0.743	1.153
6	0.756	0.715	1.153
7	0.708	0.645	1.093
8	0.735	0.686	1.122
14	1.373	1.321	1.315
15	1.662	1.524	1.348
16	1.230	1.208	1.358
18	0.800	0.775	1.104
19	1.238	1.215	1.222
20	1.198	1.182	1.328
21	0.732	0.681	1.112
22	1.100	1.095	1.144
23	1.721	1.562	1.339
24	1.070	1.068	1.241
Average	0.993	0.939	1.178
Building	1.177	1.163	----

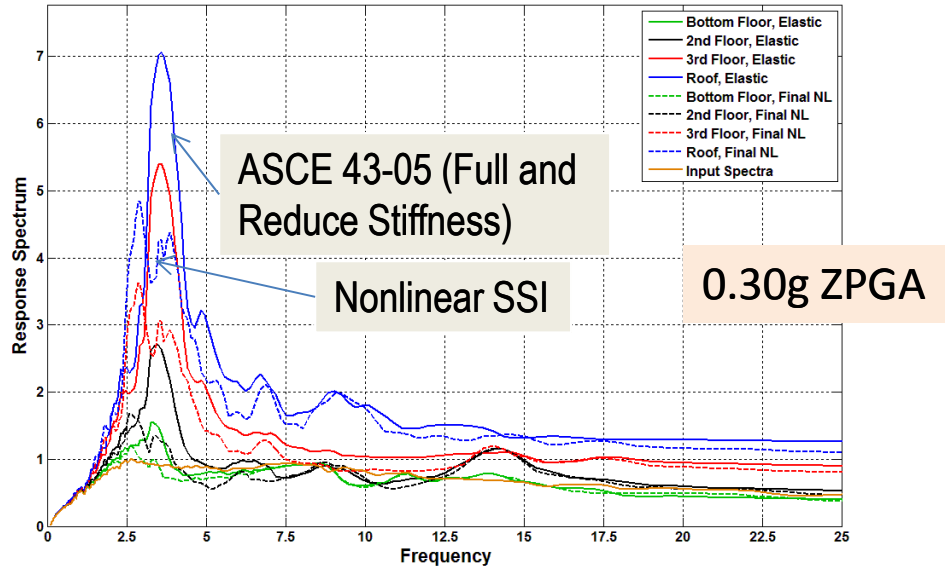
0.70g ZPGA Review Level (LS-A)

Panel Number	ASCE 43		Calcs
	μ , Final Analysis	$F\mu$, Final Analysis	$F\mu$, Shear
1	1.811	1.619	1.697
2	1.673	1.532	1.636
3	1.615	1.493	1.703
4	1.716	1.559	1.846
5	1.720	1.562	1.985
6	1.596	1.480	2.022
7	1.515	1.425	1.901
8	1.621	1.497	1.887
14	4.500	2.828	2.040
15	6.390	3.432	2.052
16	3.810	2.573	2.143
18	2.020	1.743	1.801
19	4.523	2.836	1.819
20	4.058	2.668	2.031
21	1.648	1.515	1.855
22	3.745	2.548	1.752
23	6.764	3.539	2.046
24	3.143	2.299	1.982
Average	2.993	2.119	1.900
Building	3.801	2.569	----

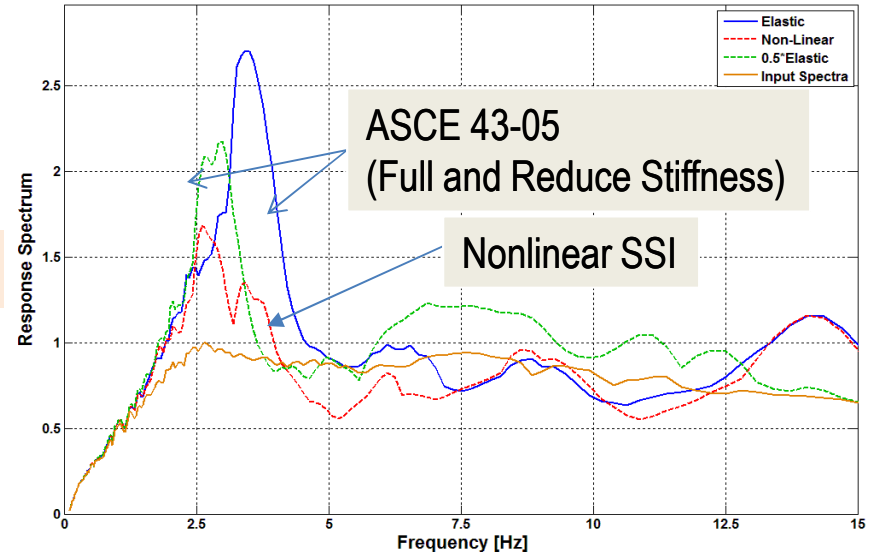
Large ductility demands

Nonlinear SSI and ASCE 43-05 Inelastic Reduction Factors

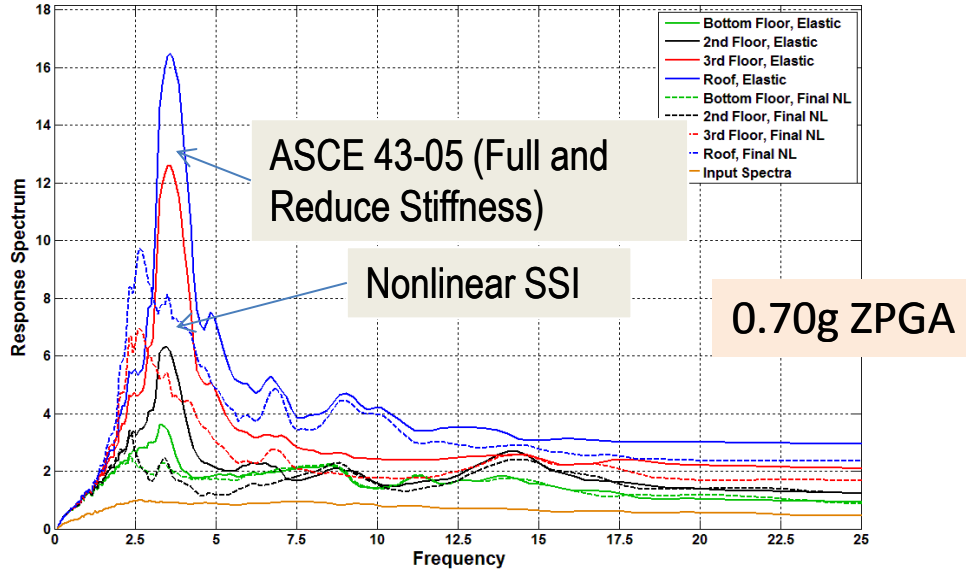
Y 0.3g Rock Base Response Spectrum Comparison, 3 Floor Side



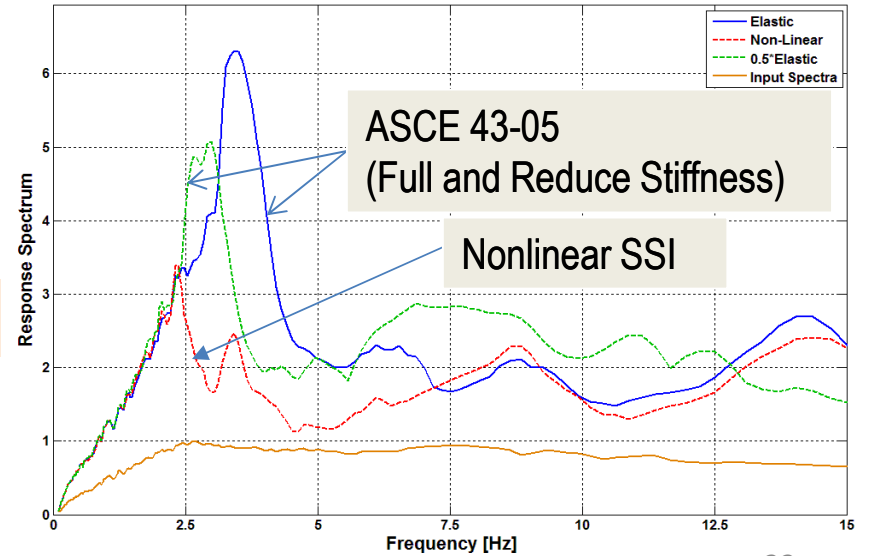
Y 0.3g Rock Base Response Spectrum Comparison, 2nd Floor



Y 0.7g Rock Base Response Spectrum Comparison, 3 Floor Side



Y 0.7g Rock Base Response Spectrum Comparison, 2nd Floor



Conclusions

- Nonlinear SSI analysis in complex frequency domain is a very promising engineering approach. It is at least 500 -1000 times faster than nonlinear SSI analysis in time domain.
- It provides results consistent with the ASCE 43-05 recommendations.
- Nonlinear SSI analysis in complex frequency is much more robust than nonlinear SSI analysis in time domain that is much more sensitive, especially for higher frequencies. Nonlinear time domain analyses are more prone to analysis errors than nonlinear complex frequency domain analyses.

The nonlinear SSI approach in complex frequency is currently implemented in the ACS SASSI Option N capability. The commercial version will be available in 2014.

The nonlinear approach is currently extended to soil material hysteretic behavior (providing more realistic results than the equivalent-linear SHAKE methodology), and to other types of structural concrete components.